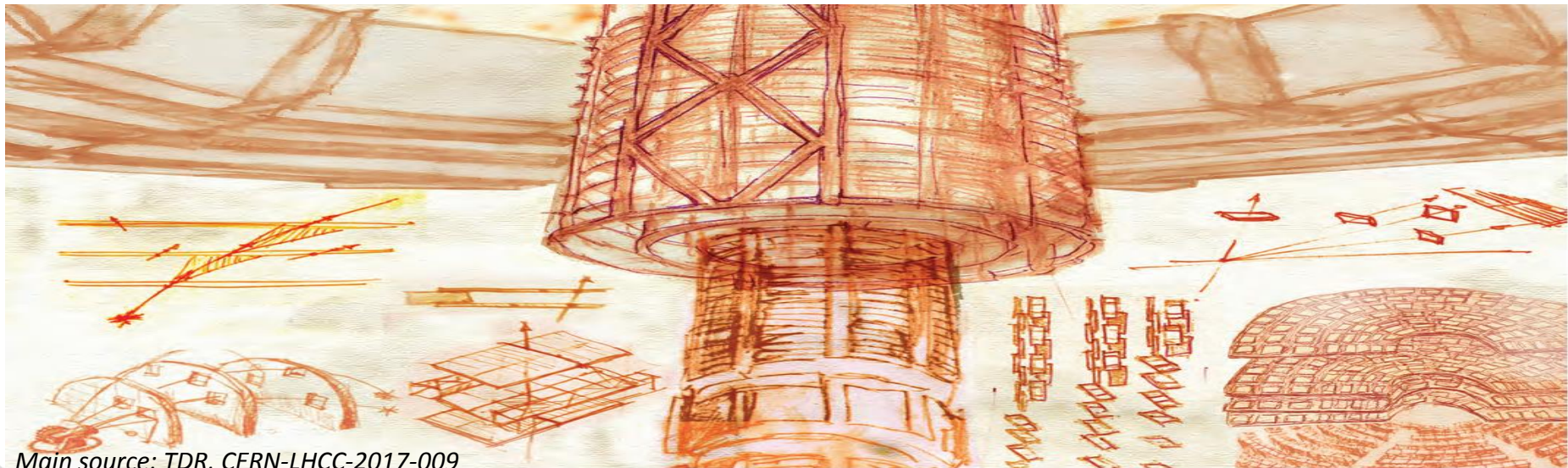


The CMS Outer Tracker for HL-LHC

Alexander Dierlamm on behalf of the CMS Tracker Collaboration

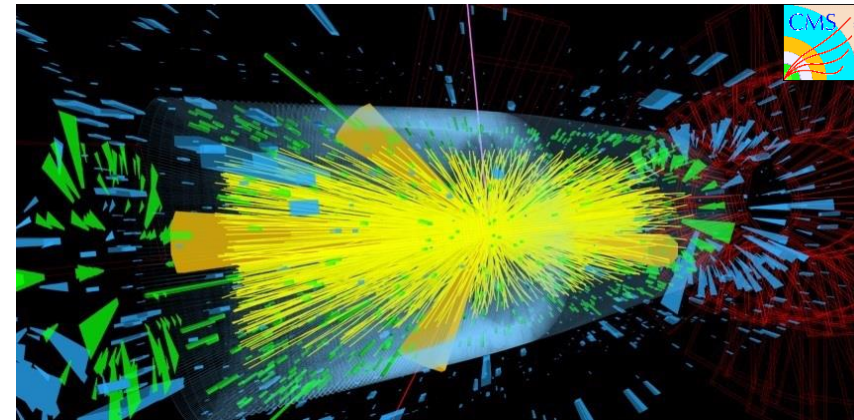
INSTITUT FÜR EXPERIMENTELLE TEILCHENPHYSIK



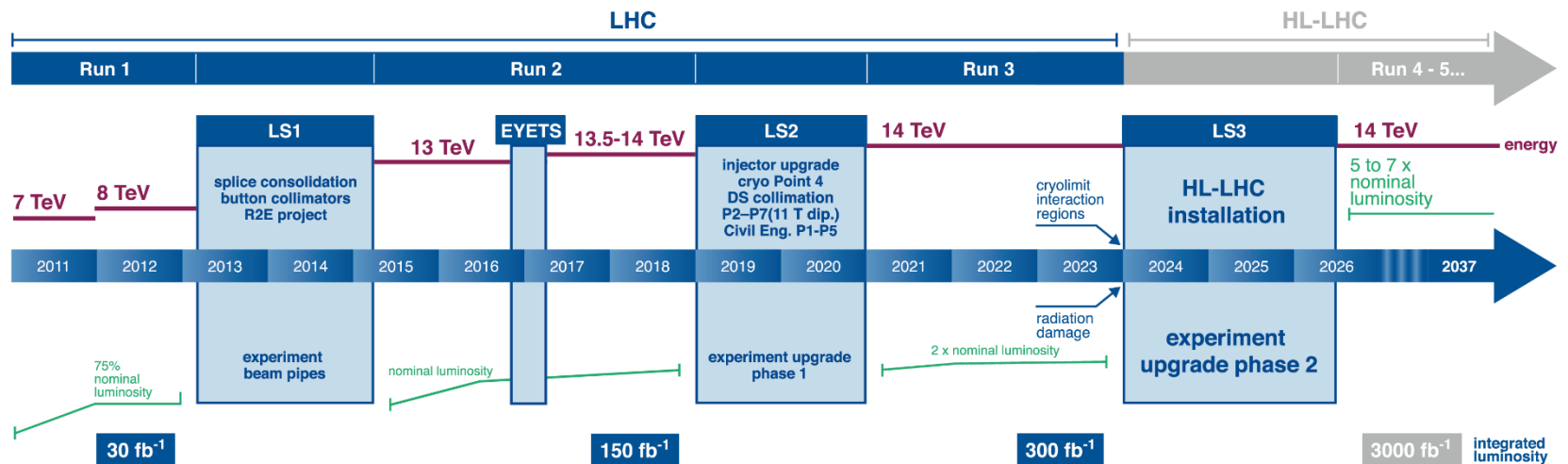
Main source: TDR, CERN-LHCC-2017-009

HL-LHC

- To extend the discovery potential
 - the luminosity will be increased by a factor of 5 (pile-up $\sim 140-200$)
 - the integrated luminosity will be increased from 300fb^{-1} to 3000fb^{-1}



LHC / HL-LHC Plan

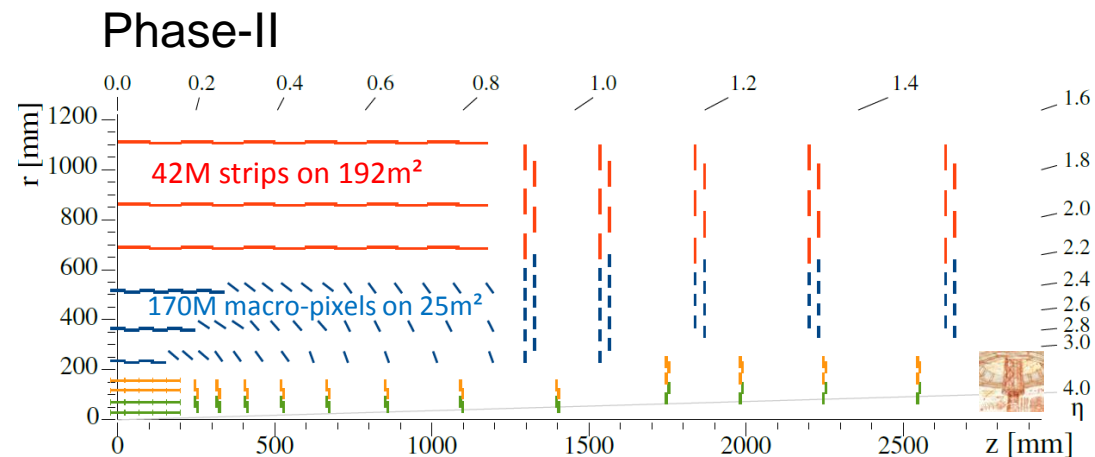
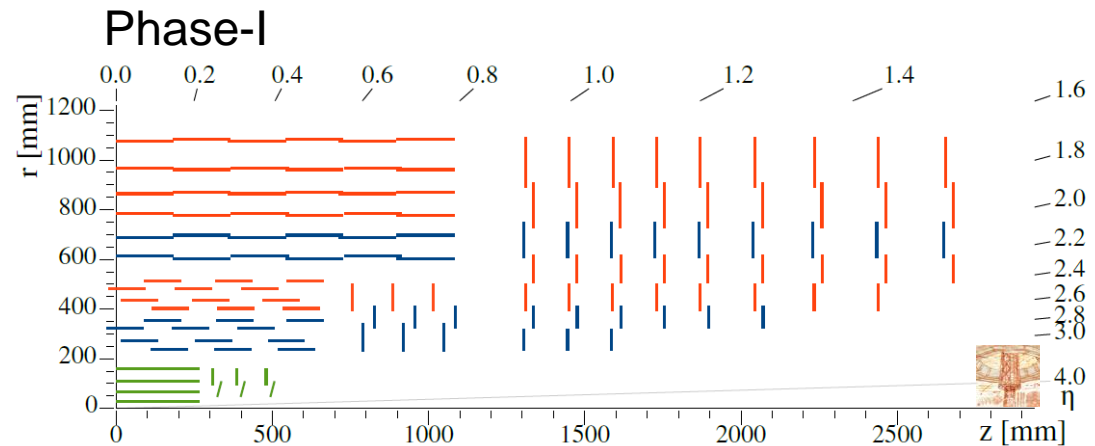


Requirements for Outer Tracker at HL-LHC

Requirement	Implementation	Buzzwords
Alive up to 3000fb^{-1}	<ul style="list-style-type: none"> Radiation resistance Cold (-20°C) operation 	<ul style="list-style-type: none"> n-in-p type silicon CO_2 cooling
$O(1\%)$ occupancy up to PU~140 (possibly more); robust pattern recognition	<ul style="list-style-type: none"> Increased granularity Optimized layout 	<ul style="list-style-type: none"> Macro-pixel sensors
Contribute to L1 trigger	<ul style="list-style-type: none"> Track trigger capabilities 	<ul style="list-style-type: none"> pT-modules
Upgraded L1 trigger: <ul style="list-style-type: none"> higher rate (750kHz) longer latency ($12.5\mu\text{s}$) 	<ul style="list-style-type: none"> Large readout bandwidth Deep front-end buffers 	<ul style="list-style-type: none"> Binary readout Gigabit links
Reduce material effects	<ul style="list-style-type: none"> Minimization/optimization of passive volumes 	<ul style="list-style-type: none"> CO_2 cooling Tilted barrel

The new Tracker Layout

- New features:
 - fewer layers
 - tilted inner barrel
 - (extended pixel)
 - modules with sandwich of 2 sensors (2 hits/module)
 - total: 13296 modules
 - macro-pixel sensors



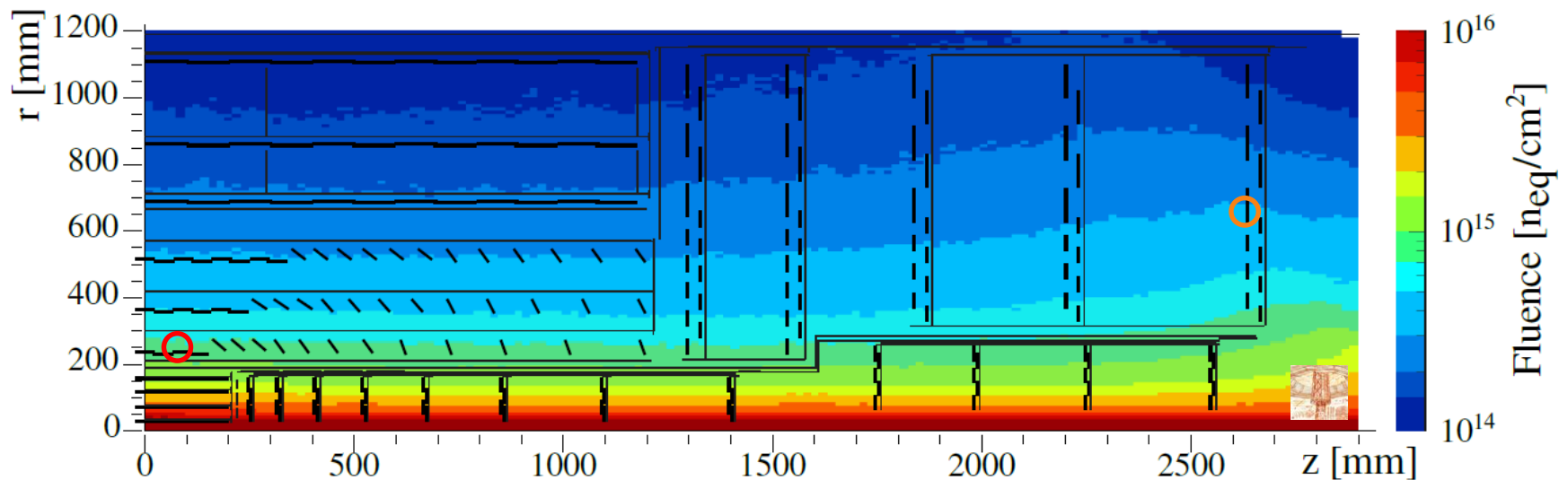
The ATLAS approach is shown on poster
 P55, Z. Liang, "Construction of the new silicon microstrips tracker for the Phase-II ATLAS detector"

2S modules: 2 Strip sensors

PS modules: Pixel and Strip sensor

Radiation Environment

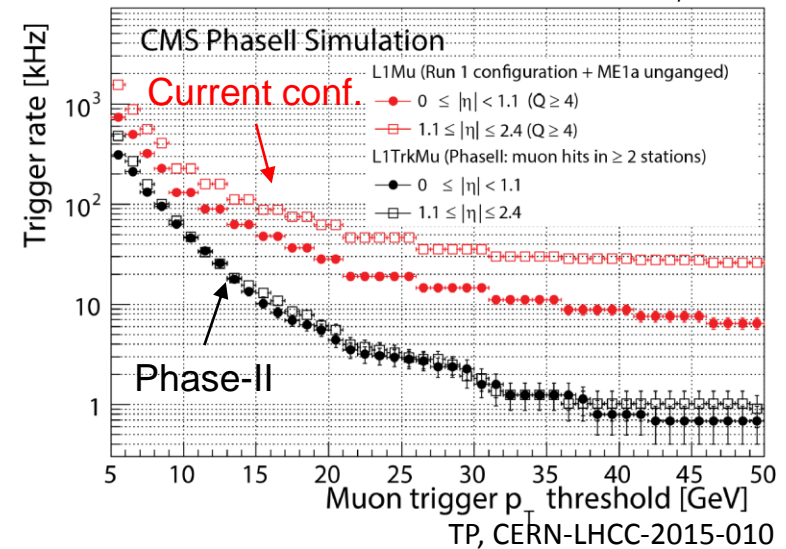
Region	max. fluence	max. dose
R>20cm (PS modules)	$1 \times 10^{15} n_{eq}/cm^2$	700kGy
R>60cm (2S modules)	$3 \times 10^{14} n_{eq}/cm^2$	10kGy



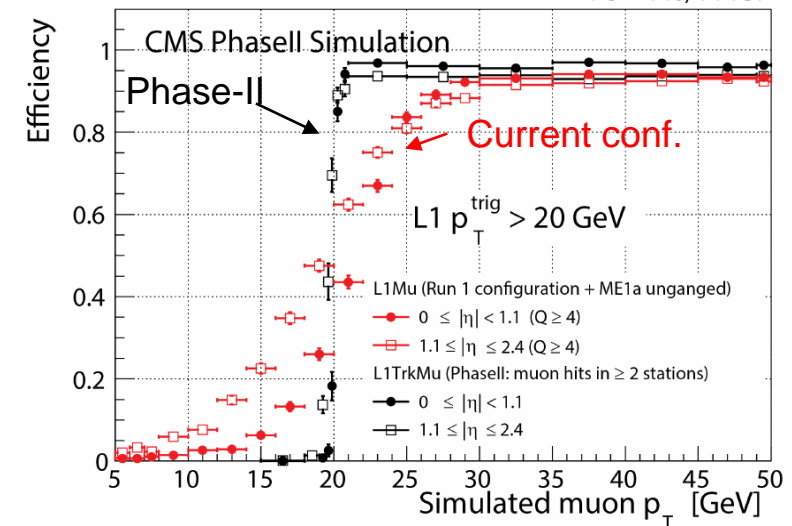
Tracks from Outer Tracker for L1-Trigger

- Tracks required to
 - keep L1 trigger rate at acceptable 750kHz
 - maintain selection efficiency
- Longer latency of $12.5\mu\text{s}$ to receive and process tracker data
- Baseline concept:
 - highly parallelized track finding and fitting on FPGA farm
 - demonstrated to find tracks within $4\mu\text{s}$
- Challenge: get data out for each bunch crossing (25ns)

PU = 140, 14 TeV

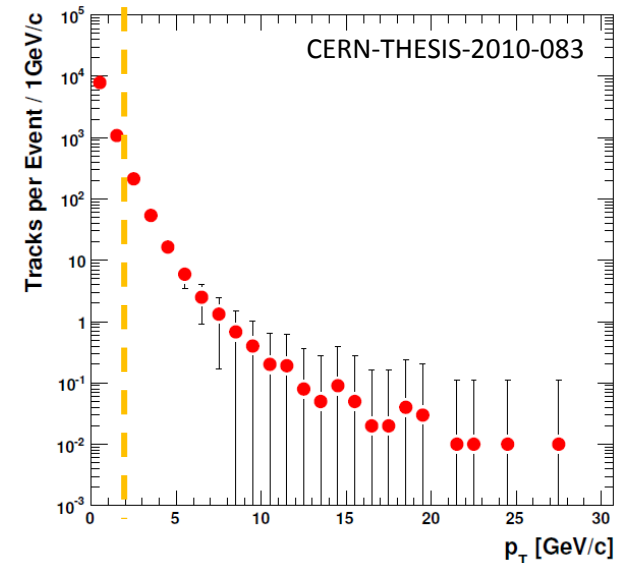


PU = 140, 14 TeV

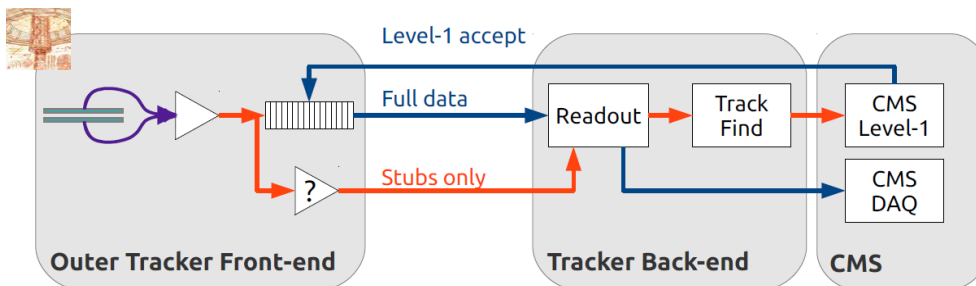


p_T Discrimination Concept

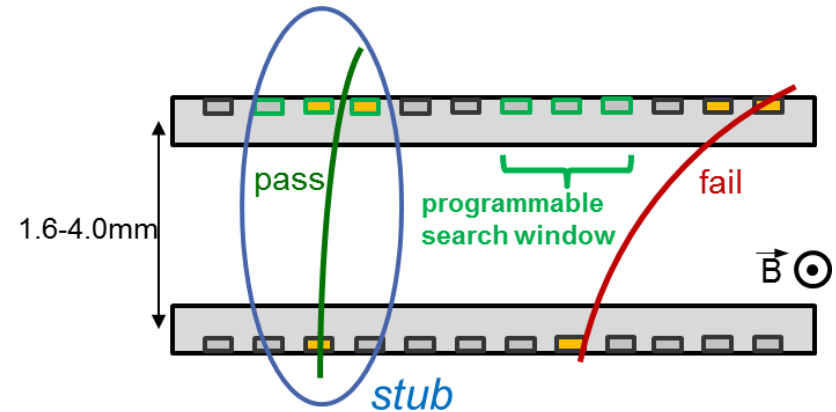
- Reduce number of relevant hits for L1 by discrimination on p_T
 - $p_T > 2 \text{ GeV}/c$ removes 99% of tracks
- Need on-module data reduction
 - modules contain two sensors with small gap
 - electronics use programmable search window to accept high- p_T tracks and form stubs (hit position + bend info)
 - stubs are read out for each BX and sent to L1 Track Finder



p_T spectrum for hits at $R=25\text{cm}$ from minimum bias particles at an average pileup of 400

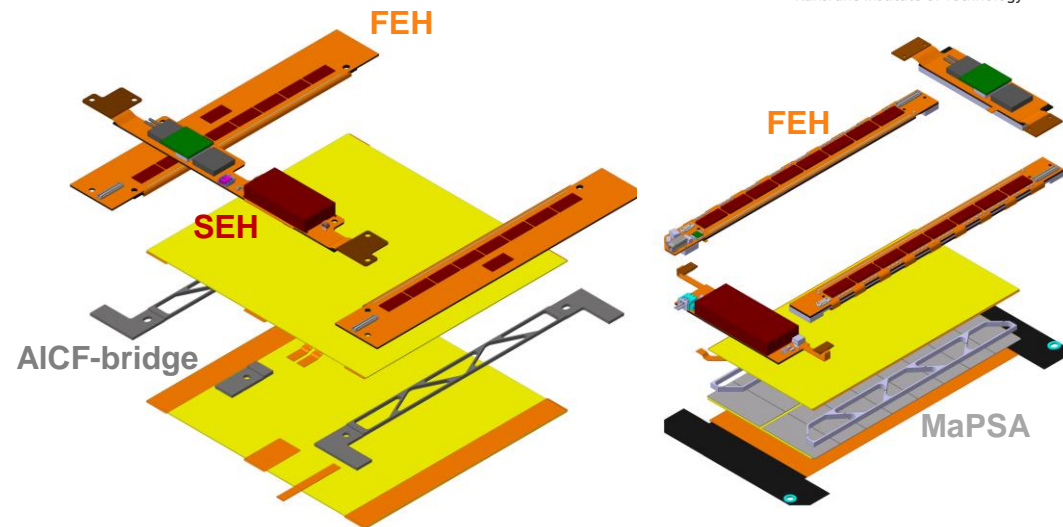


- @40 MHz rate / LHC bunch crossing
- @750kHz / CMS L1 average rate



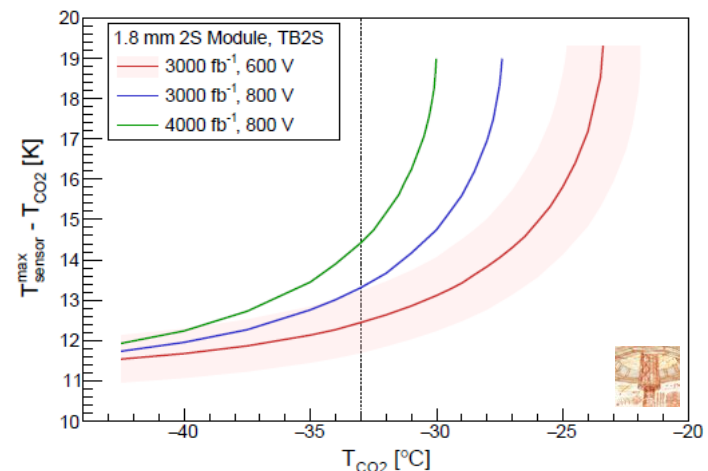
p_T Modules

- Modules are self-contained readout entities
- Parts to be assembled:
 - Front-end hybrids (FEH)
 - readout and concentrator ASICs
 - Service hybrids (SEH)
 - power and opt. comm.
 - AICF-bridges
 - high thermal conductivity and similar CTE as silicon
 - HV isolation and HV connection
- Important:
 - sensors to be well aligned (<400μrad)
 - good thermal performance
 - low material budget
 - HV stability (≤800V)



2S module

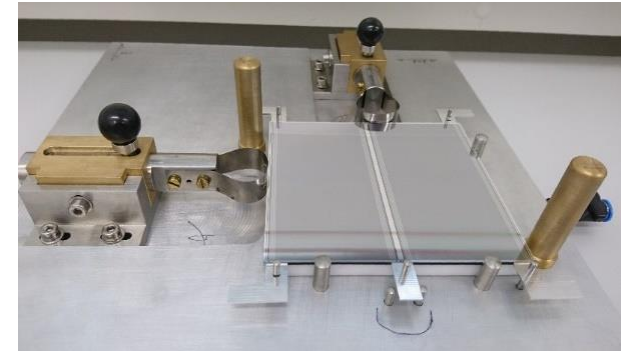
PS module



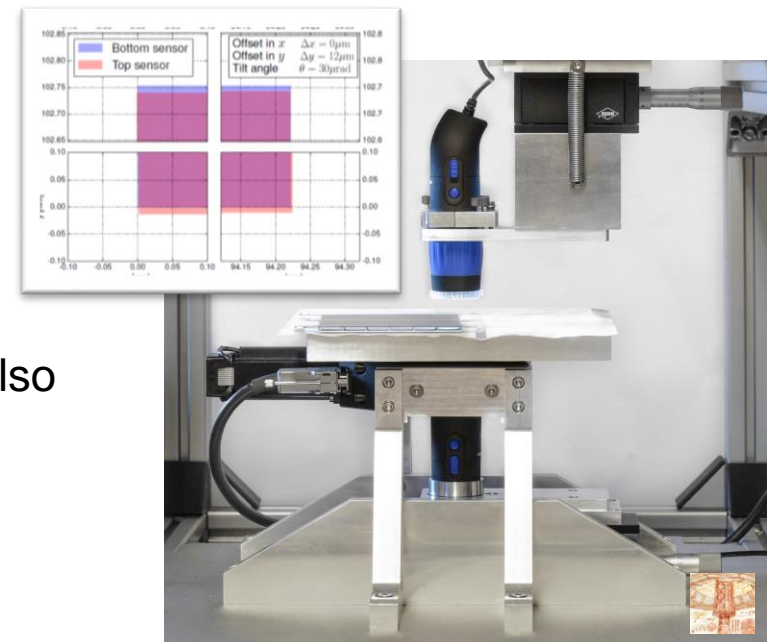
Simulation of thermal runaway for worst 2S module

Module Assembly

- Strips of two sensors need to be aligned precisely ($<400\mu\text{rad}$) to allow correct stub finding
- Manual assembly using jigs with precision stops allows rotations $<100\mu\text{rad}$
 - also requires accurate dicing of sensors
 - and tool to measure geometry
- Further crucial ingredients
 - thin glue layers (ΔT)
 - several jigs (bare module, FEHs, SEH, bonding)
 - encapsulation of wirebonds
 - cheap carrier plates ($\sim 15000\text{pcs.}$) usable also for functional tests



Bare module assembly jig at KIT



Double-sided metrology station at Aachen

The ATLAS approach is shown on posters
 P28, Carlos Garcia Argos, "Assembly and Electrical Tests of the First Full-size ForwardModule for the ATLAS ITk Strip Detector"
 P29, Peter Phillips, "Prototype Strip Barrel Modules for the ATLAS ITk Strip Detector"

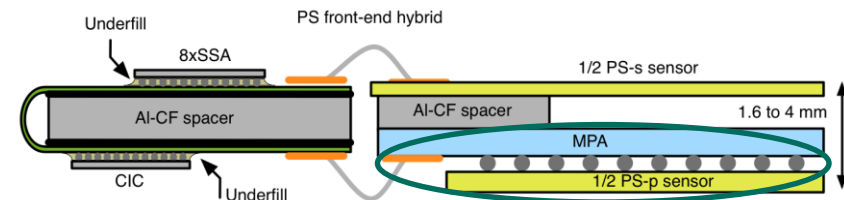
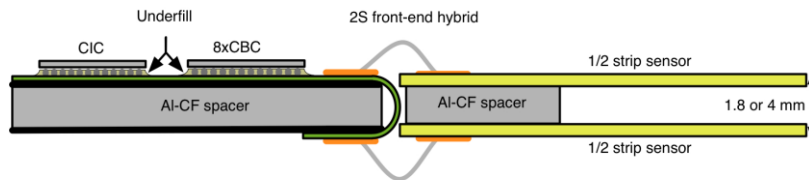
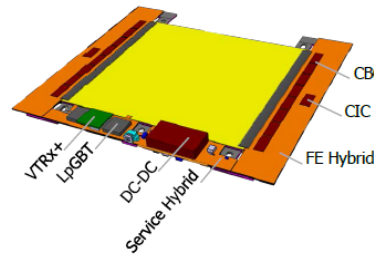
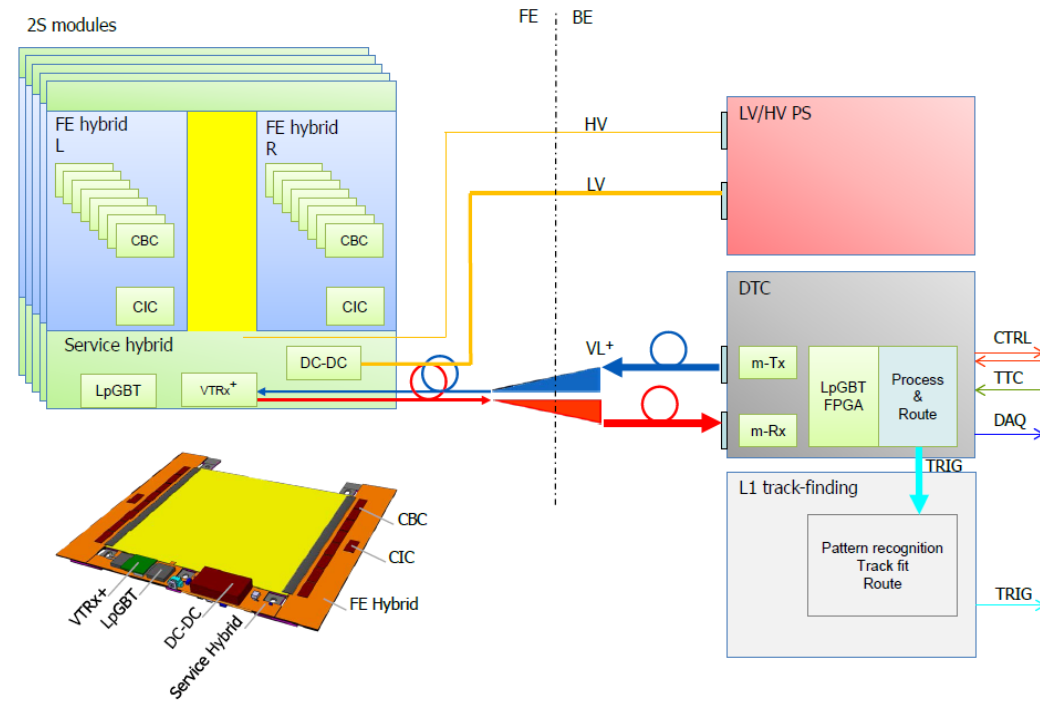
Electronic System

■ Front-end hybrids

- Readout chips (CBC/MPA) provide binary readout data and stub info (48b/BX/chip)
- CIC collects and serializes data (320Mb/s)
- Flex hybrids interconnect top and bottom side of modules

■ Service hybrids

- Gigabit Transceiver (lpGBT) drives optical link (~5Gb/s)
- DC-DC conversion for LV power (12V → 2.55V/1.25V/1.0V)

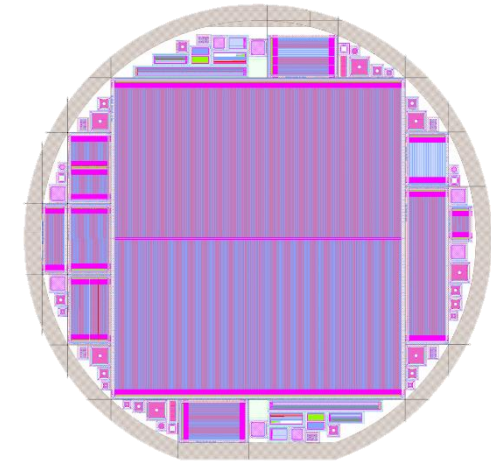


MaPSA

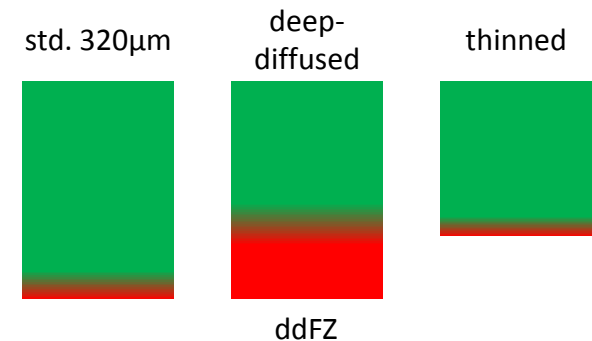
Sensors

- Three sensor types only (15 for current tracker)!
 - 15'360 x **2S strip** sensors (AC)
 - 10 x 10 cm², 90μm pitch, 5cm long strips
 - 5'616 x **PS-s strip** sensors (AC)
 - 10 x 5 cm², 100μm pitch, 2.5cm long strips
 - 5'616 x **PS-p macro-pixel** sensors (DC)
 - 10 x 5 cm², 100μm pitch, 1.5mm long macro-pixels

- Sensors will be
 - n-in-p type with p-stop or p-spray
 - High resistivity FZ, ddFZ (or mCZ)
 - Active thickness between 200 - 240 μm
 - Biased up to 800 V

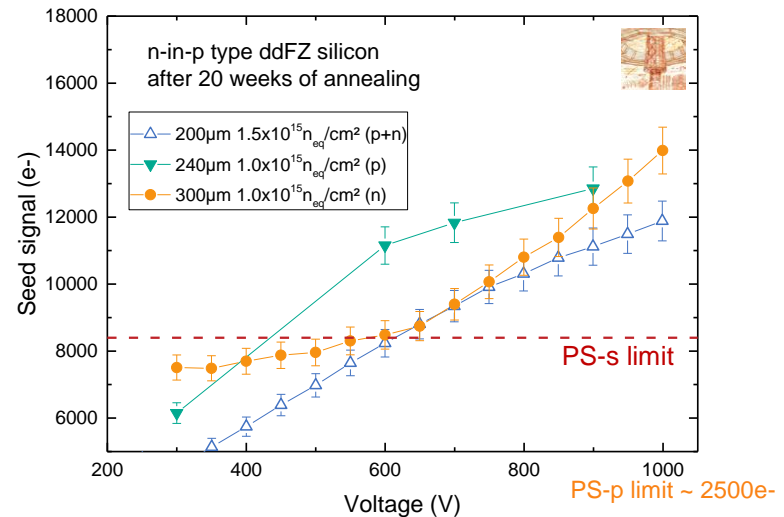
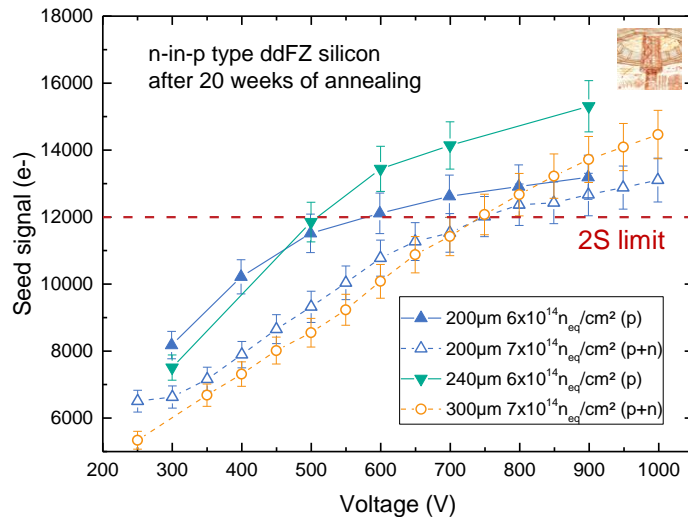
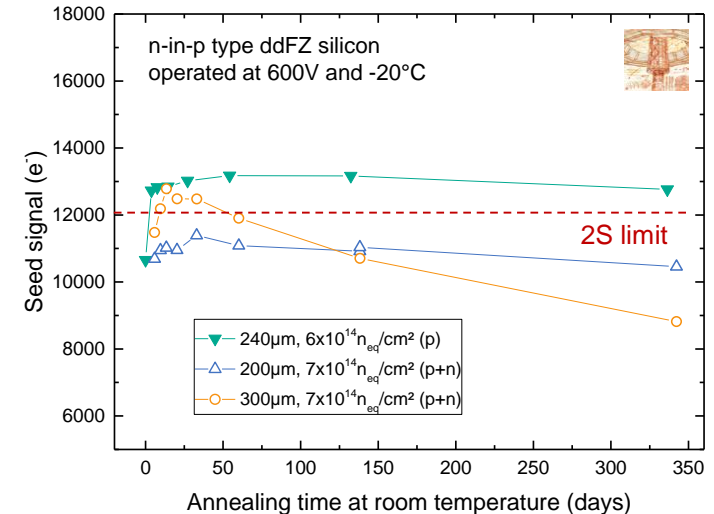


2S prototype wafer



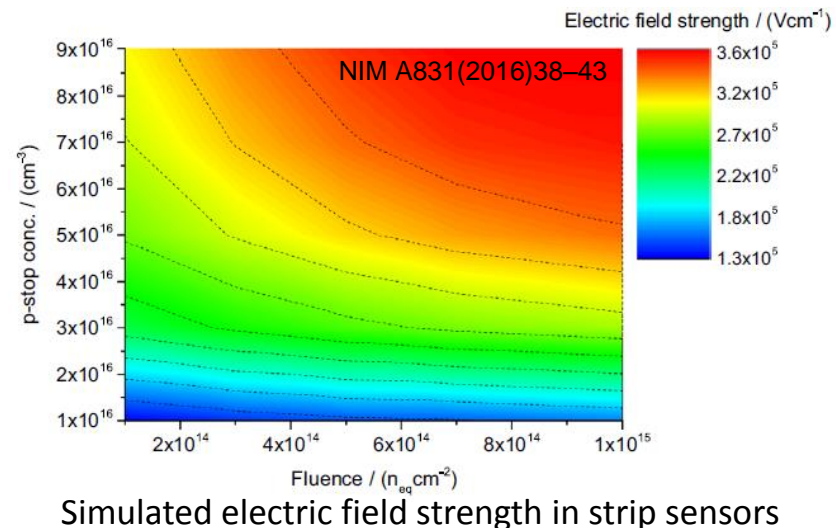
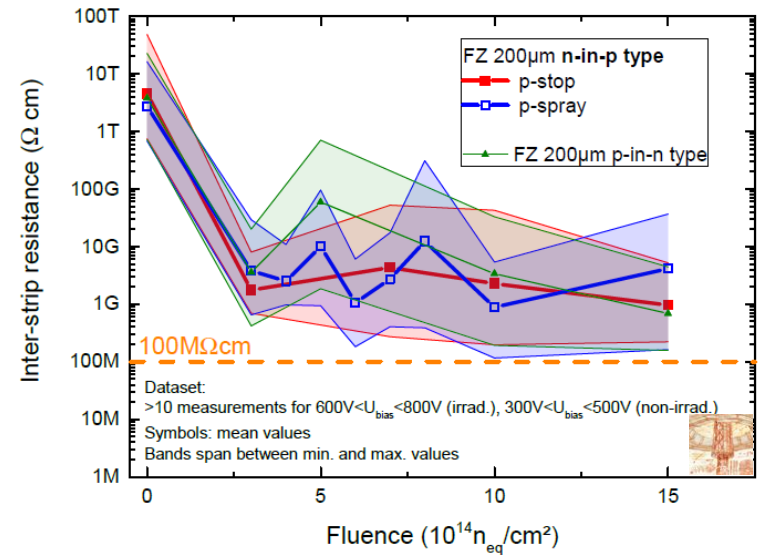
Sensors: optimal thickness

- Optimal thickness seems to be around 240µm for strip sensors (2S, PS-s)
 - stable signal at 600V vs. annealing
 - good to exploit reduction of leakage current
 - sufficient seed charge to be efficient at targeted fluence (and beyond)
- PS-p macro-pixel connected to low noise ROC → 200µm sensor thickness sufficient

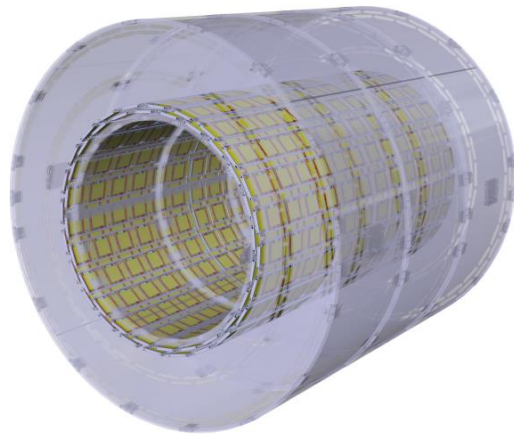


Sensors: further optimization

- Strip isolation
 - p-stop as well as p-spray process can establish sufficient inter-strip resistance
 - moderate implantation doses should be used at high fluence to avoid problems with high electric fields
- Bias rails can be improved to reduce inefficiencies
 - see e.g. poster P08, D. Schell, “Optimization of bias rail implementations for segmented silicon sensors”
- Test structure designs for fast and reliable process control
 - see e.g. poster P04, V. Hinger, “Process Quality Control of Large-Scale Silicon Sensor Productions for Future HEP Experiments”

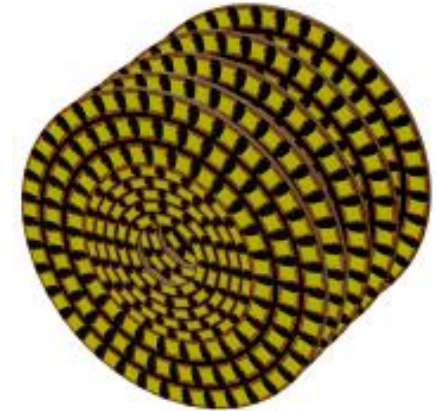
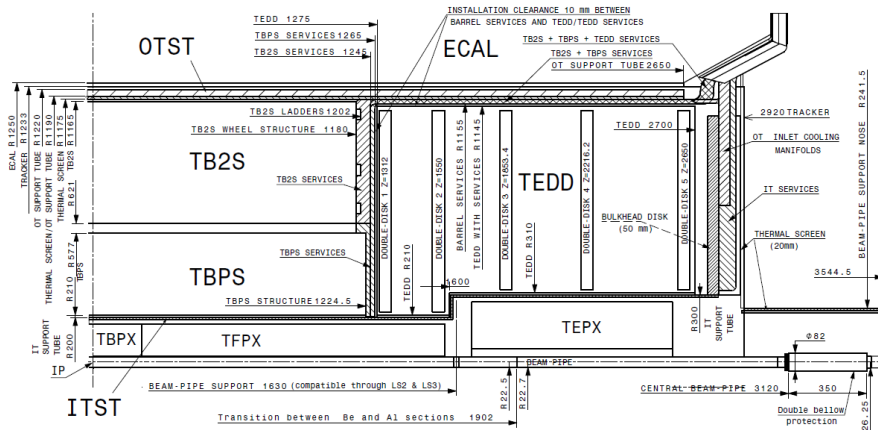


Mechanics

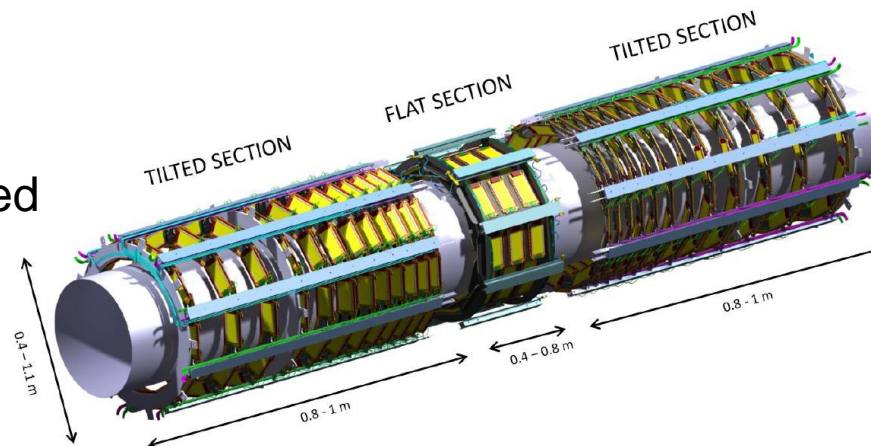


Outer barrel contains ladders with 2S modules similar to the current TK barrel

Inner barrel has tilted sections equipped with PS modules

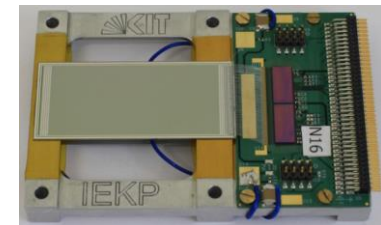


Endcaps contain dees with 2S and PS modules forming double-discs (hermetic coverage)

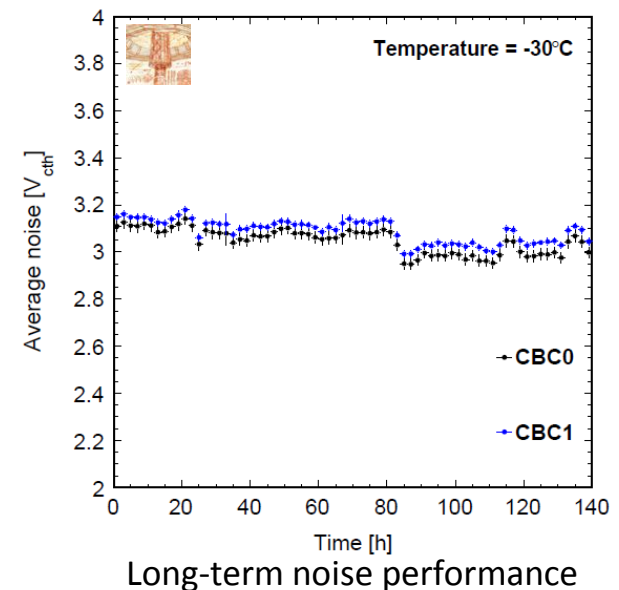
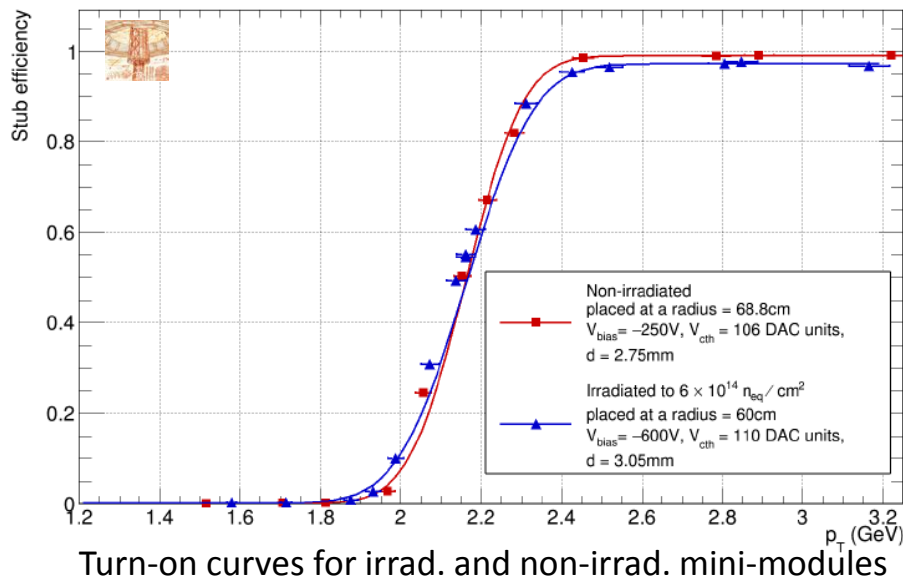


Prototyping: 2S mini-module

- Dual-CBC hybrid connected to two small sensors
- Non-irradiated and irradiated mini-module operated at CERN SPS
 - pT discrimination validated (curvature of track emulated by rotating module wrt. beam)
- Long-term operation showed flat noise
- Most recent version of CBC with full functionality arrived lately, see next talk

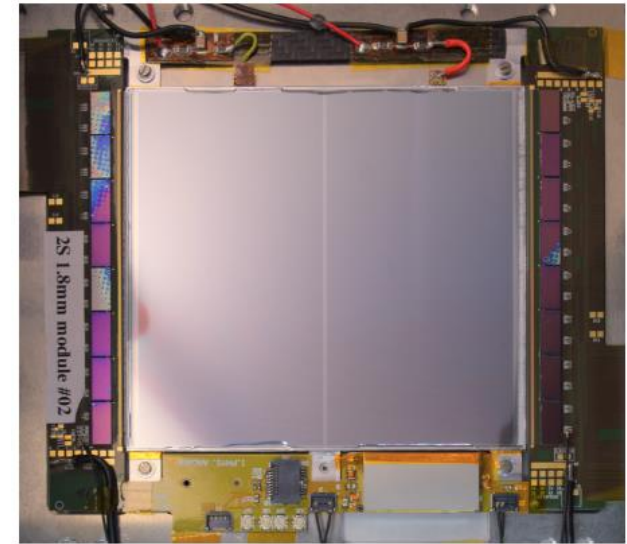


2S mini-module

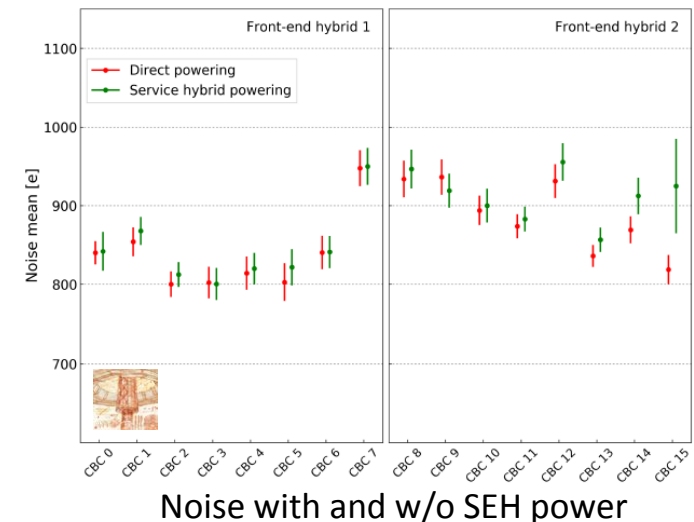
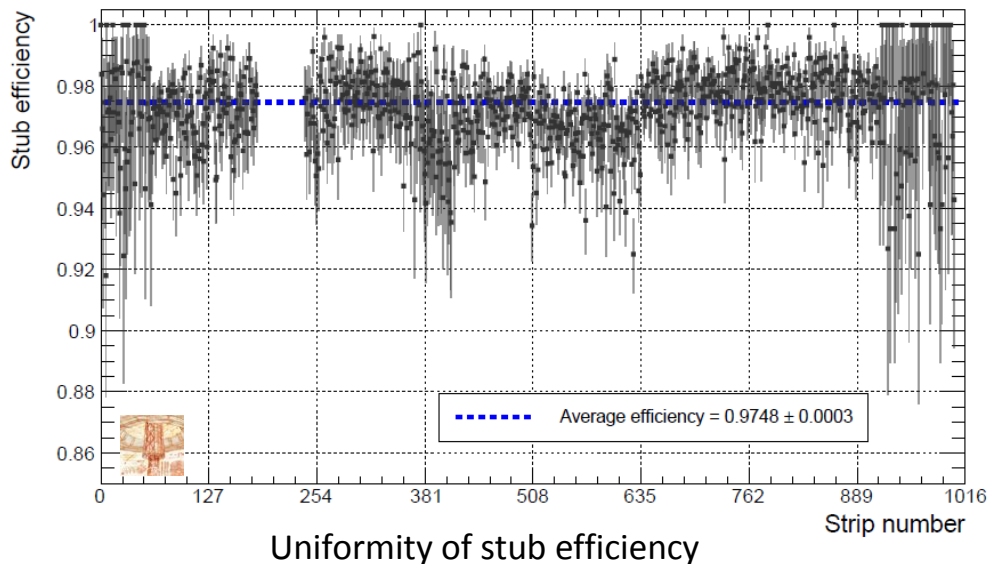


Prototyping: 2S module

- Full-size 2S modules operated in beam
 - uniformity and pT discrimination validated
- Operation with DCDC converter showed only minor increase in noise close to the coils

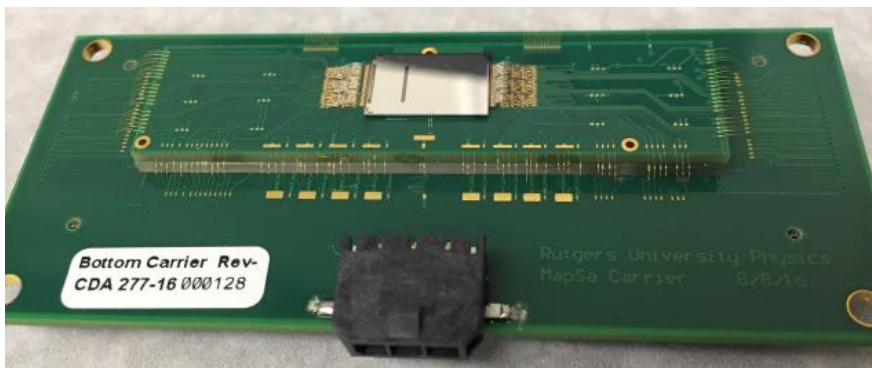
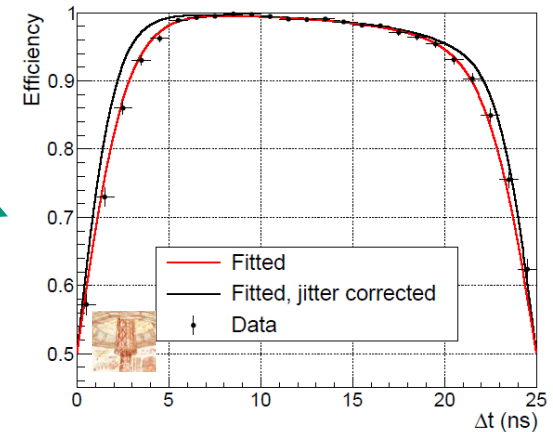
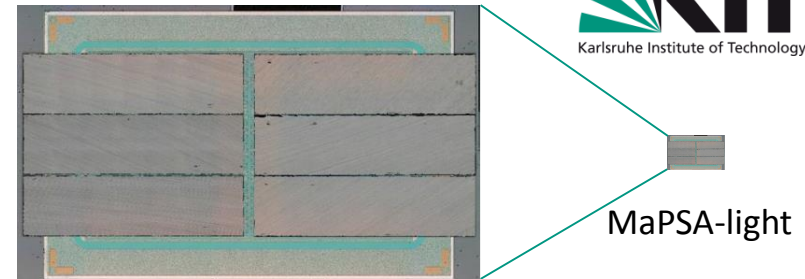


2S module with DCDC converter

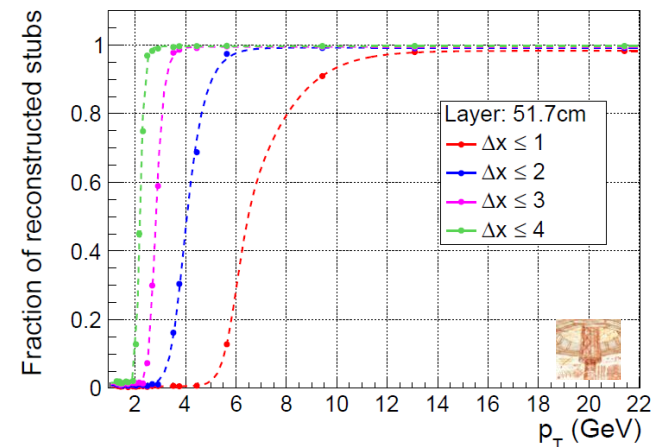


Prototyping: MaPSA

- 6 small prototypes of MPA bump-bonded to small macro-pixel sensor forms micro version of MaPSA
- Test analogue functions of MPA
 - e.g. efficiency vs. clock phase shift
- Test bump bonding and HV isolation
- Also PS micro-module was assembled
 - discrimination functional
- Imminent: full-size MPA chip

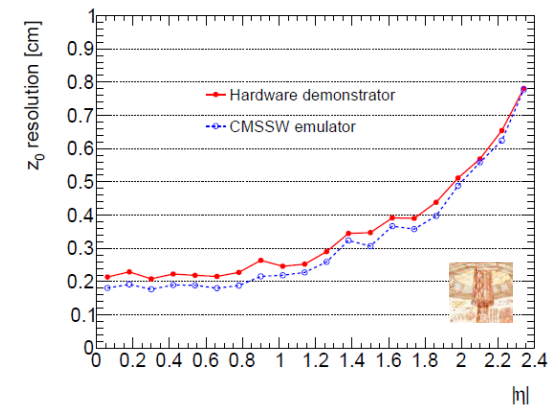
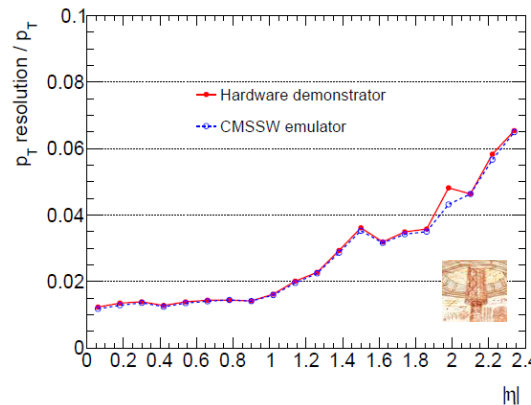
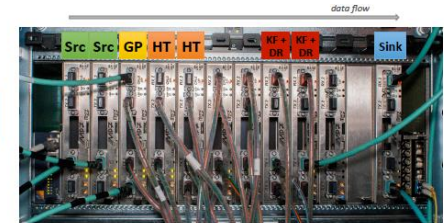
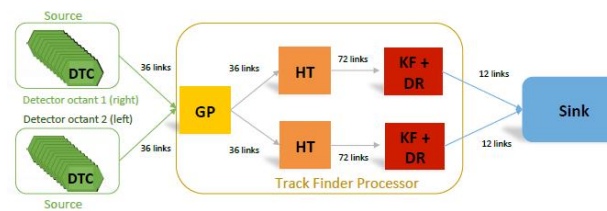
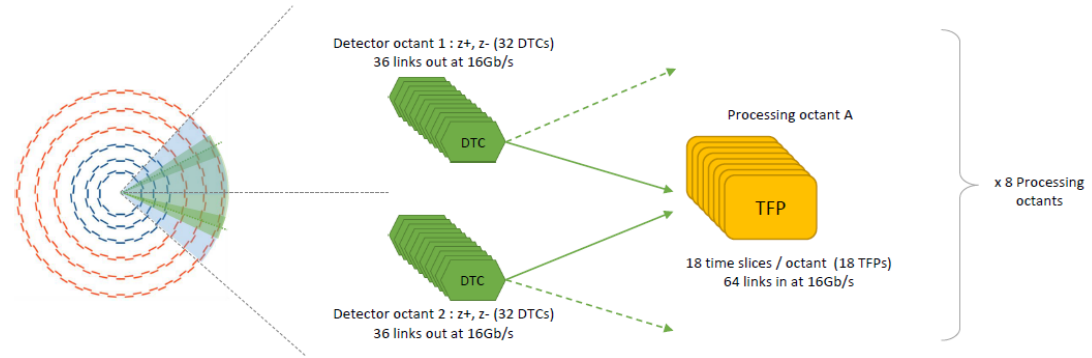


PS micro-module



L1 Track Finder: Demonstrators

- Parallel processing of geometric sectors and time slices
- Two baseline approaches using FPGAs:
 - Hough transform →
 - Tracklets
- Both demonstrated latency $< 4\mu\text{s}$ and good performance
- Alternative: AM chips see poster P37, R. Rossin, "A Track Finder with Associative Memories and FPGAs for the L1 Trigger of the CMS experiment at HL-LHC"



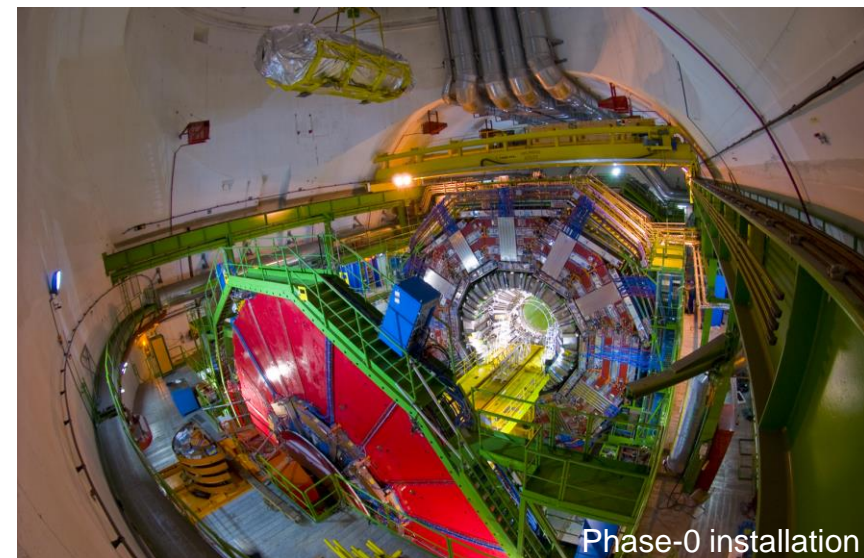
HT performance in tt + 200 PU events

Outlook

- All concepts of CMS Outer Tracker validated
- TDR approved (CERN-LHCC-2017-009)
- Need to ramp-up prototyping and focus on production

Date	Some selected milestones
Aug.17	Proto MPA/SSA submission ✓
Jan.18	First CIC proto submission
May.18	OT Power system concept defined
Jan.19	CIC final proto submission
Aug.19	OT sensors production submission
Dec.19	CBC production submission
...	...

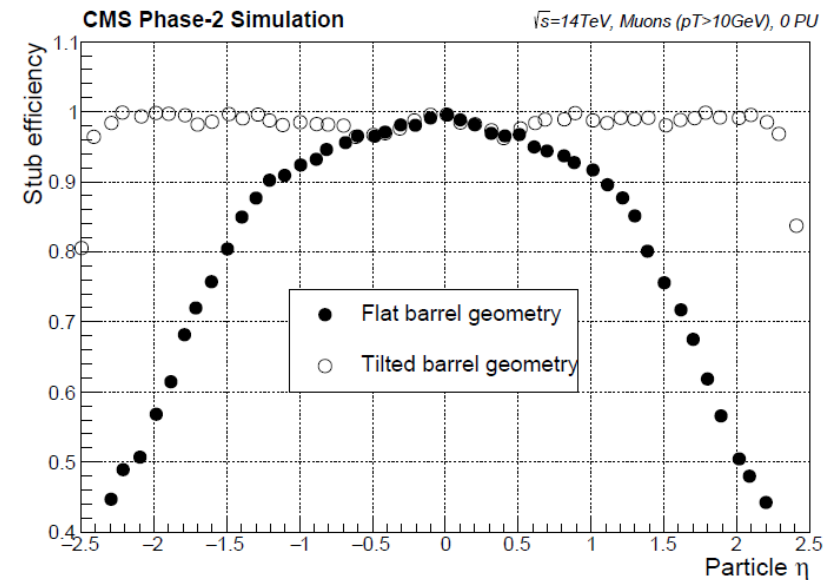
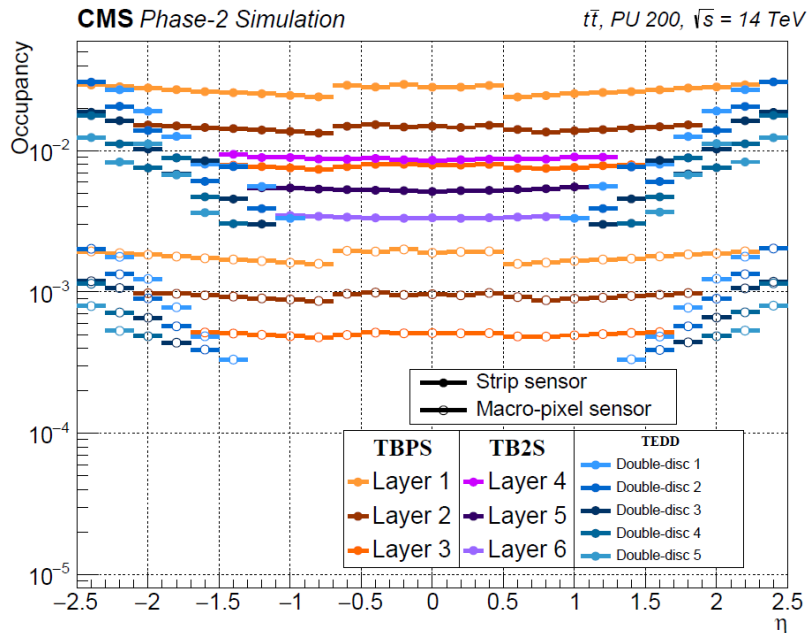
Pre-production: 2020-2021
 Production: 2021-2023/24
OT installation: 2025



Phase-0 installation

SPARES

Performance: Occupancy, stub efficiency



Performance: Tracking

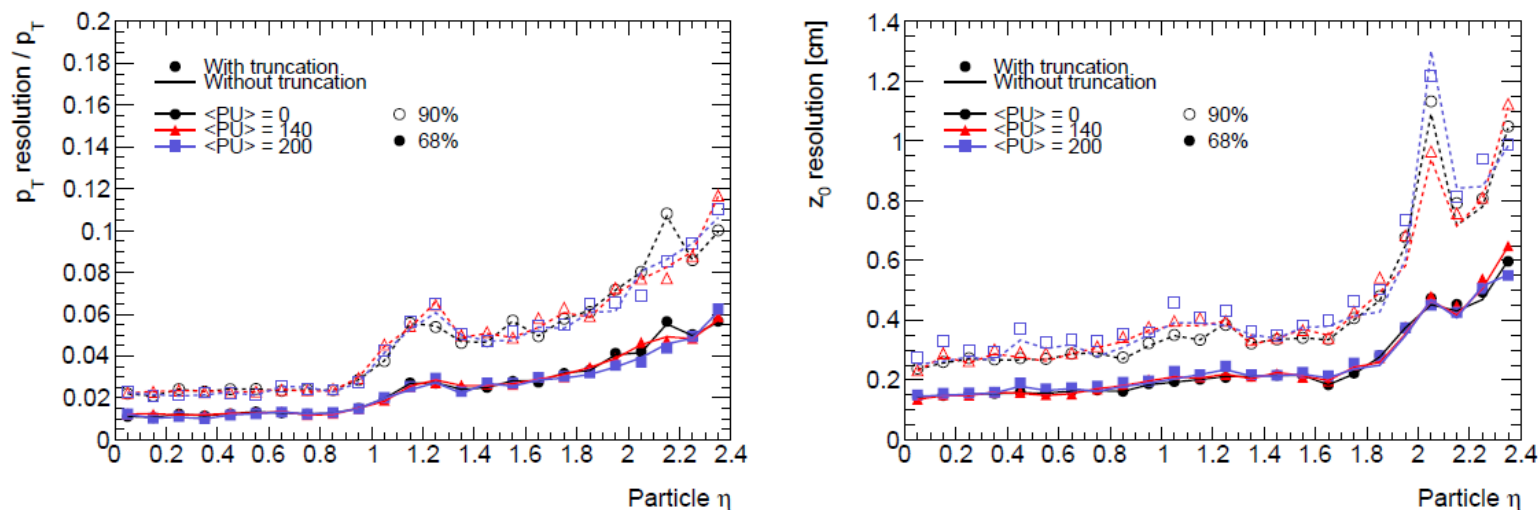
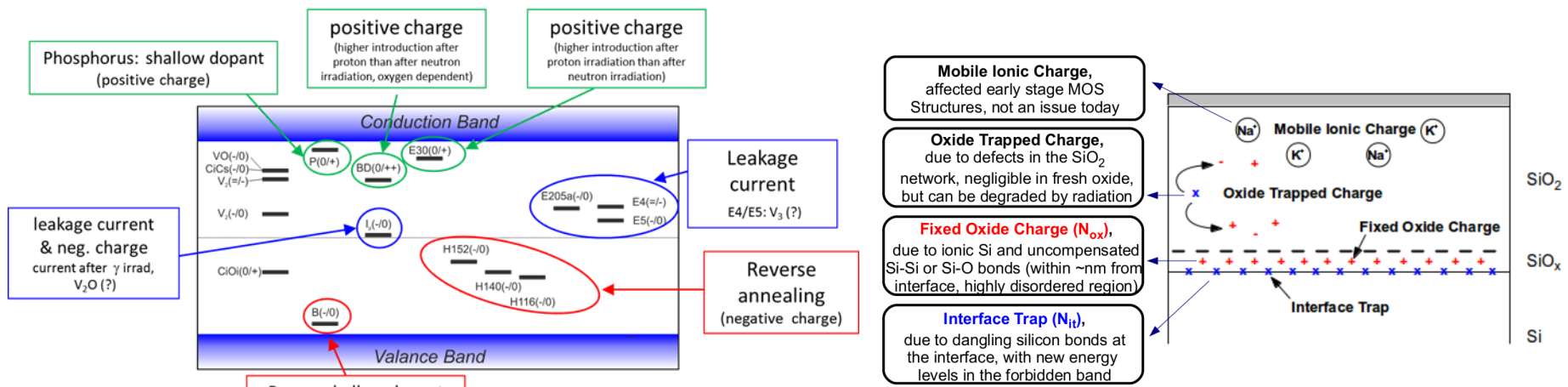


Figure 6.8: Relative p_T resolution (left) and z_0 resolution (right) versus pseudorapidity for muons in $t\bar{t}$ events with zero (black dots), 140 (red triangles), and 200 (blue squares) pileup events on average. Results are shown for scenarios in which truncation effects are (markers) or are not (lines) considered in the emulation of L1 track processing. The resolutions correspond to intervals in the track parameter distributions that encompass 68% (filled markers and solid lines) or 90% (open markers and dashed lines) of all tracks with $p_T > 3$ GeV.

Radiation Damage

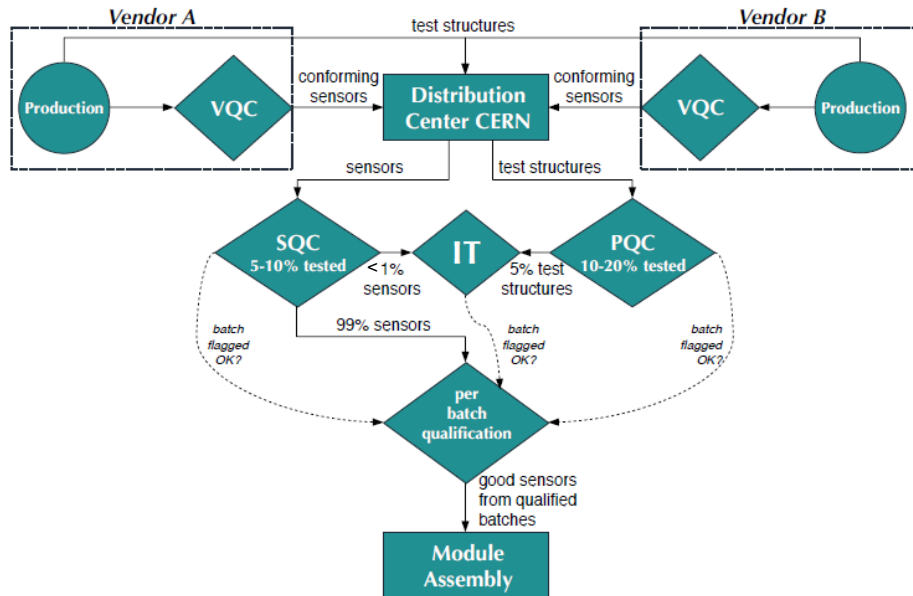
- Bulk damage
 - Primary lattice defects (I and V) form higher order defects (V_2 , VO , ...) or even defect clusters, with energy levels in the band gap of Si
 - Depending on energy level and cross section they contribute to
 - leakage current, effective doping concentration, trapping
- Surface damage
 - Ionizing radiation generates e/h pairs also in SiO_2
 - e much higher mobility than h \rightarrow positive charge up of oxide
 - Additional, interface traps with dynamic characteristics
 - These lead to
 - increased surface currents, altered electric field in surface region, accumulation of electrons at surface



M. Moll, VERTEX13

J. Zhang, PhD, DESY, 2013

Sensor QC



Measurement type	Acceptance value/window	Measured at			
		VQC	SQC	PQC	IT
Global measurements (2S, PS-s, and PS-p)					
Full depletion voltage	$V_{fd} < 150 \text{ V}$ for $200 \mu\text{m}$ $V_{fd} < 300 \text{ V}$ for $300 \mu\text{m}$	✓	✓	✓	✓
Current at 500 V	$I_{500} \leq 2 \text{ nA/mm}^3$	✓	✓	✓	✓
Breakdown voltage	$V_{break} > 700 \text{ V}$, $I_{700} < 3 \times I_{500}$	✓	✓	✓	✓
Longterm stability	$ \Delta I_{500}/I_{500} < 30\%$ for 48 hours	-	✓ ¹	-	-
Measurements after irradiation (2S, PS-s, and PS-p)					
Breakdown voltage	$V_{break} > 1000 \text{ V}$, $I_{1000} < 4 \times I_{700}$	-	-	-	✓
Interstrip resistance	$R_{int} > 100 \text{ M}\Omega\text{cm}$	-	-	-	✓
Strip measurements (2S and PS-s)					
Strip current	$I_{strip} \leq 2 \text{ nA/cm}$	✓	✓	-	✓
Bias resistor	$\text{median}(R_{poly}) = 1.5 \pm 0.3 \text{ M}\Omega$	✓	✓	✓	-
median per sensor	$R_{poly} = \text{median}(R_{poly}) \pm 5\%$	✓	✓	-	-
per strip		✓	✓	✓	✓
Coupling capacitance	$C_{ac} > 1.2 \text{ pF}/(\text{cm } \mu\text{m})$	✓	✓	✓	-
Interstrip resistance	$R_{int} > 10 \text{ G}\Omega\text{cm}$	-	✓ ¹	✓	✓
Interstrip capacitance	$C_{int} < 1 \text{ pF/cm}$	-	✓ ¹	✓	✓
Pinhole check	$I_{diel} < 1 \text{ nA}$ at 10 V	✓	✓	-	-
Number of bad strips	$N_{bs} < 0.5\%$	✓	✓	-	-
incl. open/shorted strips		✓	✓	-	-
Macro-pixel measurements (PS-p)					
Pixel current	$I_{pixel} \leq 300 \text{ pA/cm}$	-	-	✓	-
Interpixel resistance	$R_{int} > 1 \text{ G}\Omega\text{cm}$	-	-	✓	-
Number of bad pixels	$N_{bp} < 0.2\%$	-	-	-	-
Measurements on dedicated teststructures					
Strip/pixel implant resistivity	$R_{strip} < 250 \Omega/\text{square}$	-	-	✓	-
Strip/pixel alu resistivity	$R_{alu} < 25 \text{ m}\Omega/\text{square}$	-	-	✓	-
Dielectric breakdown	$V_{diel} > 150 \text{ V}$, $I_{diel} < 10 \text{ nA}$ at 150 V	-	-	✓	-

¹ Only for a smaller sample of sensors, approximately 1% of the full quantity.

Shielding of air coils for DCDC convertors

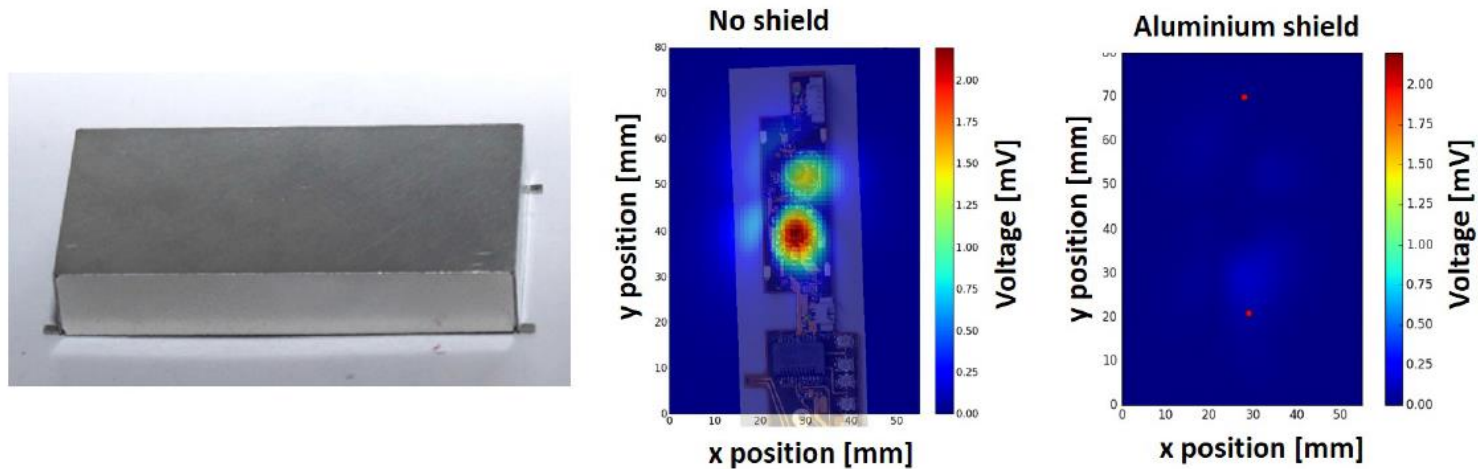
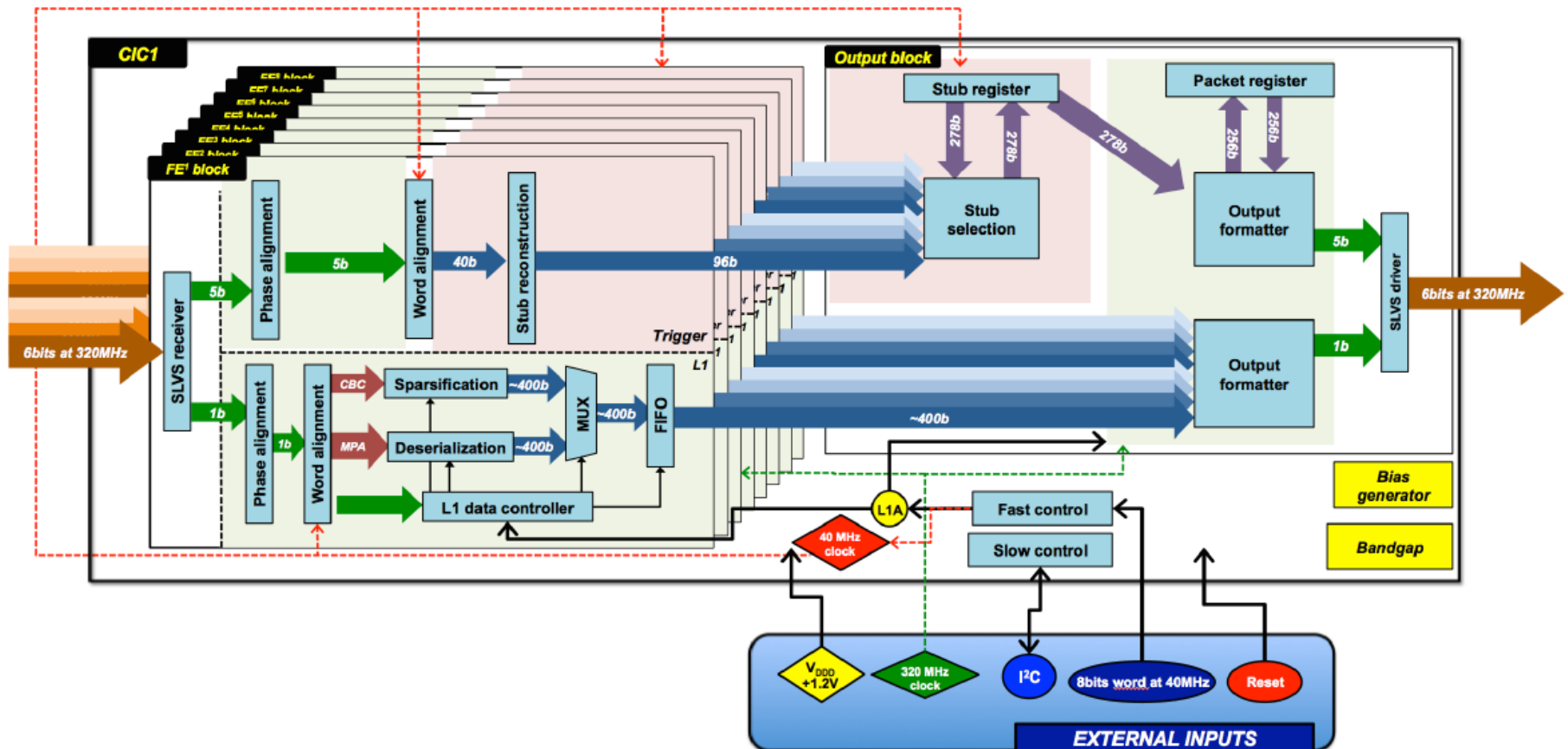


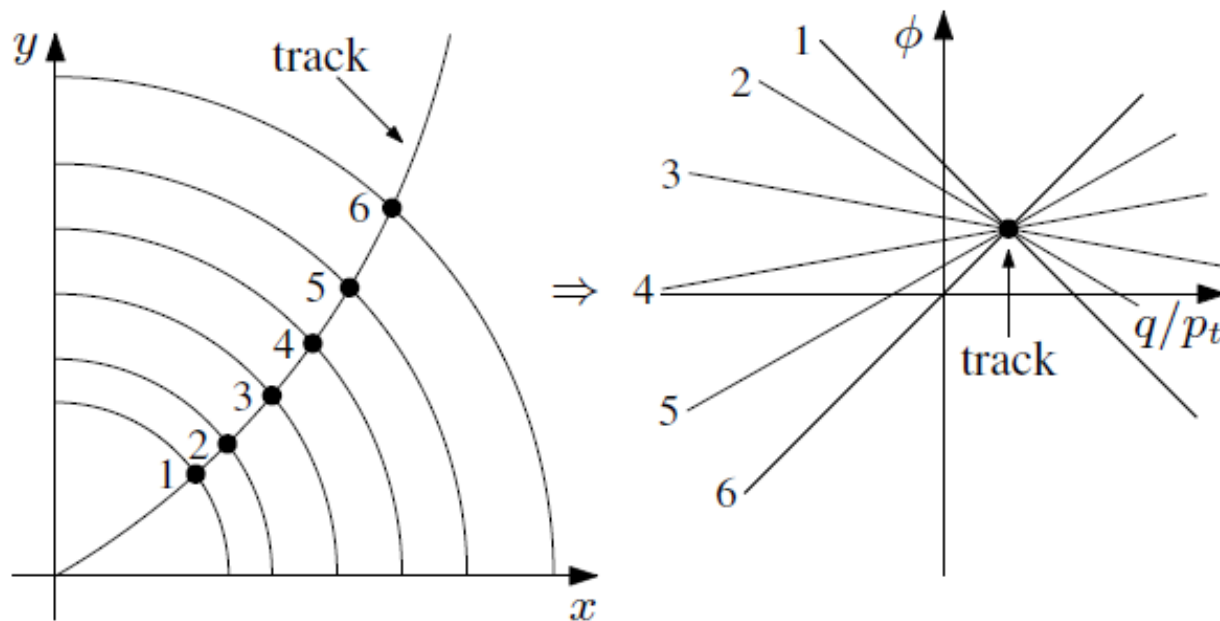
Figure 9.37: Left: photo of the aluminium shield. Centre and right: scan of the magnetic field, measured in millivolts. The maximum measured emission is plotted in a two-dimensional representation, where x and y refer to the axes of the scan table. The centre plot shows a measurement without shield, while the right plot was measured with the aluminium shield mounted. A photograph is superimposed onto the centre plot to illustrate where the emissions originate from. The small red dots represent alignment marks used to position the SEHs and to superimpose the photograph.

CIC block diagram



Hough transform

- Transforms track into point in $\Phi - q/p_T$ space



$$\phi = \phi - \frac{0.57 q}{p_T} \cdot r$$

Module Quantities and Fluences

Module type and variant		TBPS	TB2S	TEDD	Total per variant	Total per type
2S	1.8 mm	0	4464	2792	7256	7680
	4.0 mm	0	0	424	424	
PS	1.6 mm	826	0	0	826	5616
	2.6 mm	1462	0	0	1462	
	4.0 mm	584	0	2744	3328	
Total		2872	4464	5960	13296	

Region or component	Max. fluence [$n_{\text{eq}}/\text{cm}^2$]	r [mm]	z [mm]
IT barrel layer 1	2.3×10^{16}	28	0
IT barrel layer 2	5.0×10^{15}	69	0
IT barrel layer 4	1.5×10^{15}	156	89
IT forward, ring 1	1.0×10^{16}	51	252
IT service cylinder	1.3×10^{15}	170	260
OT PS modules	9.6×10^{14}	218	129
OT 2S modules	3.0×10^{14}	676	2644